

A STRUCTURAL STUDY IN THE BELGIAN ARDENNES WITH SECTIONS CONSTRUCTED USING COMPUTER-BASED METHODS

C.W. LANGENBERG¹⁾, H.E. RONDEEL²⁾ & H.A.K. CHARLESWORTH¹⁾

ABSTRACT

Langenberg, C.W., H.E. Rondeel & H.A.K. Charlesworth (1977). A structural study in the Belgian Ardennes with section constructed using computer-based methods. *Geol. Mijnbouw*, 56, p. 145-154.

A 50 km² area in the eastern part of the Hercynian Dinant synclinorium of the Belgian Ardennes containing sandstones, carbonates and shales is macroscopically folded and cut by several faults. Using numerical procedures the area was divided into five domains within which the folding is statistically cylindrical. The domains were examined with the aid of structural cross-sections. Each section was constructed using a computer-plot showing the positions of outcrops projected parallel to the fold-axis onto the plane of section, together with the traces of bedding. A composite plot was obtained for all five domains by first rotating four domains separately so that their fold-axes became parallel to the fold-axis in the fifth domain. Such rotations, which affect the coordinates of outcrops as well as the direction cosines of bedding-poles, can be accomplished by matrix multiplication. Sections constructed in this way, particularly the composite section, display the structure to considerable depths. The competent rock-units within the map-area have been deformed into rounded parallel folds. The intervening incompetent units appear to be zones of disharmony especially in the south. Several south-dipping listric thrust-faults can be discerned in the sections.

INTRODUCTION

In a recent article (Charlesworth *et al.*, 1976) several numerical statistical methods for measuring and displaying the geometry of macroscopic cylindrical folds were described. Among these procedures were those for (a) identifying domains within which folding can be considered statistically cylindrical, (b) calculating orientations of fold-axes and axial planes, and (c) preparing right and oblique structural cross-sections with the aid of computer-constructed plots. While attempting to apply these methods to some folded rocks in the Remouchamps area of the Belgian Ardennes, we decided that some new procedures should be developed to deal with areas consisting of not one but several cylindrical domains. This article therefore consists of three parts: the

first summarizes the geology of the Remouchamps area, the second examines the numerical procedures employed and the third describes the results of applying these methods to the Remouchamps area.

GEOLOGY OF THE REMOUCHAMPS AREA

In the Dinant synclinorium in the Ardennes of Belgium Devonian and Carboniferous sedimentary rocks are exposed. It extends ENE from Dinant (fig. 1) for a distance of 50 km before terminating against the unconformably underlying Lower Paleozoic metasedimentary rocks of the Stavelot massif. The general fold axis of the synclinorium is essentially horizontal except where, as in the eastern half of the Remouchamps area, it plunges moderately westwards off the Stavelot massif.

The Devonian and Carboniferous strata within the Remouchamps area have been grouped into the following five rock-units: (A) Lower-Middle Devonian clastics, (B) Middle-Upper Devonian limestones, (C) Upper Devonian silstones

¹⁾ Department of Geology, University of Alberta, Edmonton, Alberta (Canada) T6G 2E3

²⁾ Geological Institute, University of Amsterdam, Amsterdam (The Netherlands)

and shales, (D) Upper Devonian sandstones and (E) Carboniferous carbonates. We have not used Fourmarier's (1954, 1958) more detailed subdivision because (of (1) the scarcity of outcrop in many places and (2) the rapidity with which facies changes occur (see e.g. Asselberghs, 1946;

Fourmarier, 1954; Bouckaert *et al.*, 1970; Coen, 1974). The relationship between the above five units and the more numerous cartographic units on the 1:25.000 Louveigné-Spa geological map (Fourmarier, 1958) is shown by means of the alphameric in the stratigraphic column (fig. 2).

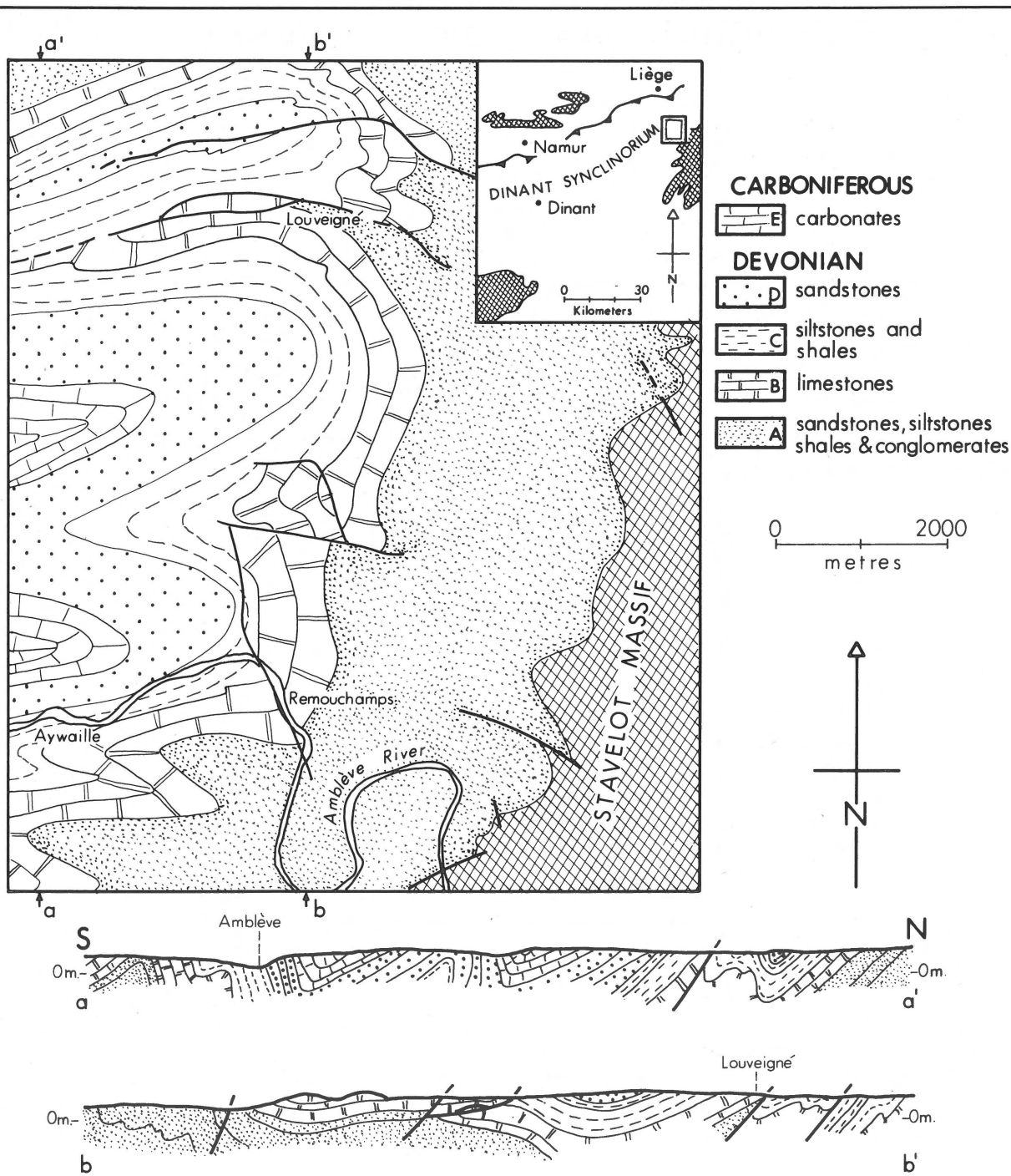


fig. 1 geological map and cross-sections of the Remouchamps area (after Fourmarier, 1958).

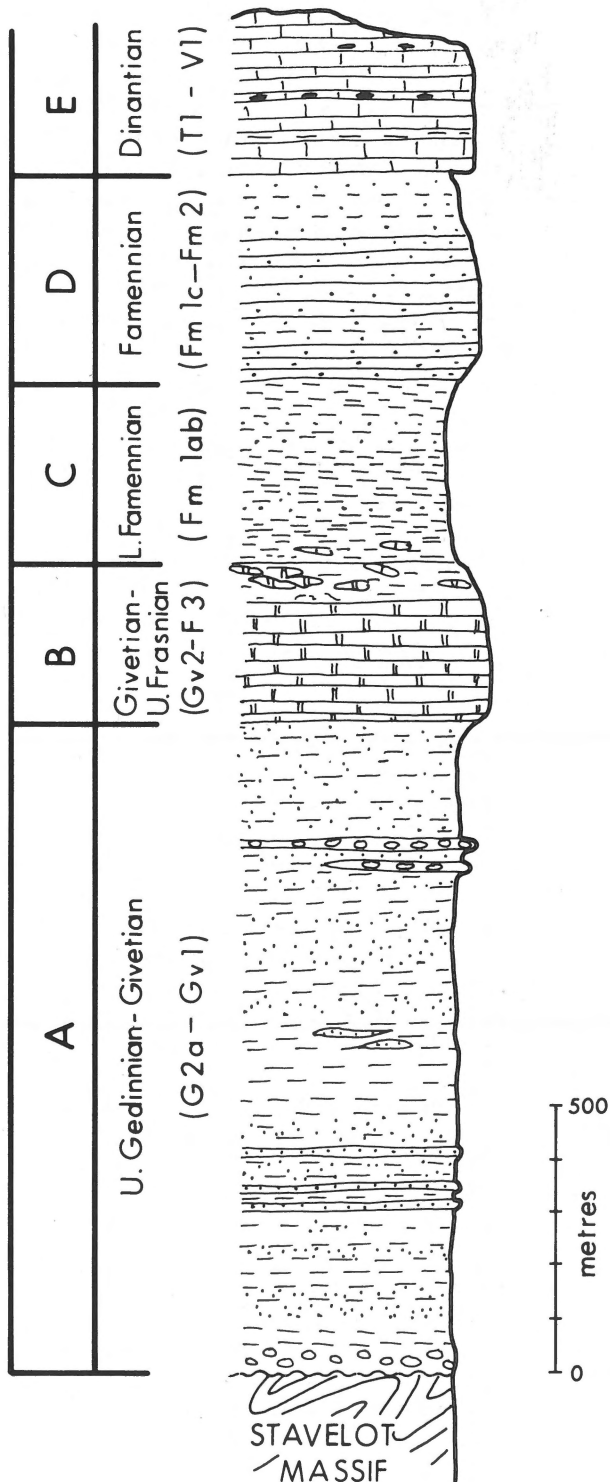


Fig. 2
Schematic stratigraphic column for the Remouchamps area (after Fourmarier, 1954, 1958).

As indicated by previously published sections (fig. 1) folding in the Remouchamps area is disharmonic, apparently the result of a zone of disharmony in the stratigraphic unit C. The axial surfaces of the folds dip to the south as do the several thrust-faults cutting units B-E. It is supposed that the faults do not continue into the more incompetent unit A (Fourmarier, 1952; cf. fig. 1).

NUMERICAL PROCEDURES

The study of folding in any area is facilitated by drawing structural cross-sections. Such sections can be constructed by projecting selected points on each folded surface s parallel to the fold-axis B from the topographic surface onto the plane of section and by joining up these points to produce smooth continuous curves. Where stratigraphic horizons cannot be accurately mapped each outcrop is projected parallel to B and represented by a short line parallel to the trace of s (fig. 3). This method of down-plunge projection, apparently developed and first applied in the Alps by Lugeon and Argand towards the beginning of the century, does not involve making any assumption as to the style of folding, although of course it assumes that the fold maintains its shape parallel to B, i.e. the fold is cylindrical in form. The method can be adapted for use with the computer by carrying out a procedure which is summarized below.

(a) The area under consideration is on inspection divided into the smallest number of subareas within which the folds appear to be cylindrical, and the orientation of the best-fit fold-axis in each subarea is calculated.

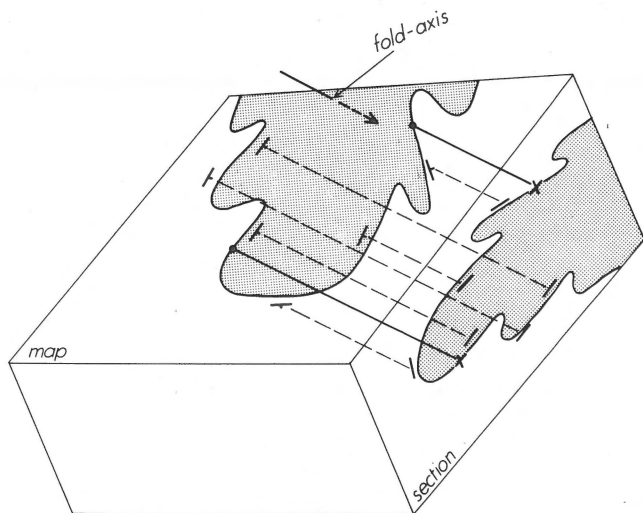


Fig. 3
Down-plunge method of constructing structural cross-sections. Where a macroscopic surface has been precisely positioned at a point on the ground, the point is projected parallel to the fold-axis onto the plane of section and represented by a cross. Outcrops not situated on such a surface are projected in a similar manner and represented by a short line parallel to the trace of the folded surface on the plane of section.

(b) The cylindricity of the folds in each subarea is tested by ascertaining whether or not the scatter of *s*-poles about the best-fit plane is within acceptable limits. On the basis of these tests subareas are grouped or subdivided into domains within which the folds can be regarded as cylindrical.

(c) The angle between the *s*-pole at each outcrop and the appropriate fold-axis is calculated and used to locate more precisely the boundaries between domains and also to reject outcrops where, probably because of error, this angle is appreciably less than 90°.

(d) The computer is instructed to prepare plots that display the projection of each outcrop as well as the trace of *s*, using as input the orientations of *s* and the coordinates of outcrops.

(e) Composite plots bringing together data from different domains are then constructed. Steps (a), (b) and (d) have already been described in some detail (C h a r l e s w o r t h *et al.*, 1976) and so will be covered only briefly in this paper.

Calculation of fold-axes

To implement numerical procedures involving orientation data, the orientation of an *s*-pole should be converted to direction cosines, i.e. the cosines of the angles that the pole makes with three mutually perpendicular axes. If these axes are due north, due east and vertically downwards, the respective direction cosines [l m n] are given by

$$[l\ m\ n] = [\cos T \cdot \cos P\ \sin T \cdot \cos P\ \sin P] \tag{1}$$

where T is the trend of the pole (in degrees azimuth) and P is the plunge (negative for upward-pointing poles specifying overturned strata). The direction cosines of the best-fit fold-axis comprise the three-element eigenvector associated with the smallest eigenvalue of the matrix T given by

$$T = \sum_{i=1}^p \begin{matrix} l_i^2 & l_i m_i & l_i n_i \\ l_i m_i & m_i^2 & m_i n_i \\ l_i n_i & m_i n_i & n_i^2 \end{matrix} \tag{2}$$

Testing cylindricity

The scatter of *s*-poles about the best-fit plane in an area may be caused by (a) personnel and instrument error in measuring *s*-poles, (b) roughness of the *s*-surfaces and (c) non-cylindricity of the folds. The null hypothesis of coplanarity of *s*-poles (i.e. of cylindricity) is rejected with confidence 1- α if

$$K \lambda_3 > \chi^2_{p-2}(\alpha) \tag{3}$$

where λ_3 is the smallest eigenvalue of the matrix T, K is the concentration parameter measuring (a) error and (b) roughness, and $\chi^2_{p-2}(\alpha)$ is the upper 100 α percentile point of the χ^2 distribution with p-2 degrees of freedom. As long as the

features producing the roughness are on a scale less than that of an outcrop K can be estimated by taking repeated measurements at an outcrop (see e.g. M a r d i a, 1972, p. 251).

If the null hypothesis of coplanarity associated with the above test is rejected, folding may still be cylindrical if the scale of the roughness features is larger than that of an outcrop. To find out whether or not this is the case, the area is divided into two segments and the matrix T compiled using data first from one segment, then from the other and finally from both segments together. The corresponding values of the smallest eigenvalues, λ_{3a} , λ_{3b} and λ_3 , are then computed. The null hypothesis of coaxiality (i.e. of cylindricity) is rejected with confidence 1- α if

$$(p-4) (\lambda_3 - \lambda_{3a} - \lambda_{3b}) / 2(\lambda_{3a} + \lambda_{3b}) > F_{2,p-4}(\alpha) \tag{4}$$

where $F_{2,p-4}(\alpha)$ is the upper 100 α percentile point of the F distribution with 2 and p-4 degrees of freedom. A probability basis for this test is given by K e l k e r & L a n g e n b e r g (1976).

If the null hypothesis associated with the F test is rejected, each segment is tested independently as above. If the null hypothesis associated with either the χ^2 or the F test is not rejected, the area may be regarded as a domain within which folding is statistically cylindrical. Finally, if the folding in adjacent areas grouped together turns out to be cylindrical, they can be amalgamated to form one domain.

Refinement of domain boundaries

The boundary between two domains may be well-defined and easy to locate: such would be the case where it is a rotational fault younger than the macroscopic folds under investigation. In other cases, however, the orientation of the fold-axis varies more gradually and the boundary has to be positioned, at least in the first instance, somewhat arbitrarily. In order to establish the boundary more precisely we proceed as follows.

The angle ϕ_i between the *i*th *s*-pole in a domain and the fold-axis B is given by

$$\cos \phi_i = l_i L + m_i M + n_i N \tag{5}$$

where [L M N] are the direction cosines of B. In an ideal correctly measured cylindrical fold this angle is invariably 90°, but in most natural cylindrical folds it is less than 90°. Once the provisional boundary between the two domains has been drawn, the fold-axes calculated, etc., the angle ϕ_i for an outcrop near the boundary is calculated using each fold-axis in turn. Clearly the domain whose fold-axis gives the larger value of ϕ_i is the one to which the outcrop should belong.

The deviation of ϕ_i from 90° can be expressed by $\cos \phi_i$ whose distribution is asymptotically normal (K e l k e r & L a n g e n b e r g, 1976). The mean of ϕ_i is zero and the standard deviation σ is given by

$$\sigma = \sum_{i=1}^p (\cos^2 \phi_i / p)^{1/2} \tag{6}$$

$$\text{Since } \lambda_3 = \sum_{i=1}^p \cos^2 \phi_i \quad (7)$$

$$\sigma = (\lambda_3/p)^{1/2} \quad (8)$$

The deviation δ_i of ϕ_i from 90° at an outcrop can thus be expressed in standard deviations as

$$\delta_i = \cos \phi_i / (\lambda_3/p)^{1/2} \quad (9)$$

Outcrops within a domain where the orientation data may be spurious, owing for example to creep, can be identified as those for which δ_i is unusually large, say greater than 2σ .

Construction of cross-sections by down-plunge projection

To write the program instructing the computer to prepare a plot that displays the projection of each outcrop as well as the trace of the folded surface s , we need to derive two sets of equations. The first transforms the coordinates of an outcrop referred to conventional east, north and vertical axes into its coordinates referred to axes parallel to the strike of the section (X), parallel to the dip of the section (Y), and normal to the section (Z): of these, the X and Y coordinates position the projection of each outcrop in the plane of section. The second set of equations expresses the pitch of the trace of s on the plane of section in terms of the orientations of s , the fold-axes B and the plane of section.

Let C be a $3 \times p$ matrix whose columns are the coordinates of the p outcrops referred to conventional axes. Then TC, the same matrix with coordinates referred to XYZ axes, can be obtained through premultiplying C by R, a 3×3 matrix whose rows are the direction cosines of the XYZ axes. The

pitch of the trace of s on the plane of section is the arctangent of l'/m' , where l' and m' are the direction cosines of the s -pole referred to axes X and Y, respectively. These direction cosines are derived through premultiplying the conventional direction cosines (in columns) by the first two rows of the matrix R. Where the desired plane of section is oblique to B, the coordinates of an outcrop referred to the X and Y axes of the section, have to be changed to $[X' - L'Z'/N' \ Y' - M'Z'/N']$ where $[L' \ M' \ N']$ are the direction cosines of B referred to axes $[X \ Y \ Z]$ and $[X' \ Y']$ are the coordinates of the outcrop referred to the X and Y axes.

Composite sections

Where an area consists of two or more domains, we may wish to construct a composite section across the entire area. If each domain has one boundary that lies on a straight line across the area (fig. 4a), the procedures summarized above may be used to obtain a series of plots, one per domain, that display the projections of each outcrop and the trace of the folded surface s on say a vertical plane through the straight line. There are several disadvantages to this method. (1) Bearing in mind that the direction of projection is different for each domain, the plots have to be prepared separately and pieced together manually. (2) Each plot will generally be on a plane oblique to the fold-axis B and the degree of obliquity will vary from plot to plot. (3) The angles between the plane of section and the fold-axes may be small, in which case the resulting sections would give a highly distorted view of the folds. Observe that if a domain does not have a boundary on the straight line across the area (fig. 4b) and the above procedure is applied, outcrops in that domain have to be projected for a certain distance in a direction that is not parallel to the appropriate orientation of B. Because of the above disadvantages and because few areas can be expected to have a common boundary, the above procedure should be modified as follows.

A single computer plot may be obtained for an area only if the direction of projection is constant throughout. Clearly if the area consists of say five domains this can be achieved only by rotating four domains independently so that their fold-axes end up having the same orientation as the fold-axis in the fifth domain. Once this has been done the whole area may be regarded as a single domain and treated exactly as described above. These rotations, which involve both s -poles and coordinates, are carried out by transforming coordinates as follows.

Consider the rotation of a domain so that its fold-axis B_1 becomes parallel to B_2 , the fold-axis of an adjacent domain. This rotation should take place about an axis A that is normal to the plane containing B_1 and B_2 (fig. 5). The direction cosines of A can be obtained by normalizing the outer product of the direction cosines of B_1 and B_2 . Similarly the direction cosines of C_1 and C_2 which are both normal to A and at right angles to B_1 and B_2 , respectively, can be found by normalizing the outer products of the direction

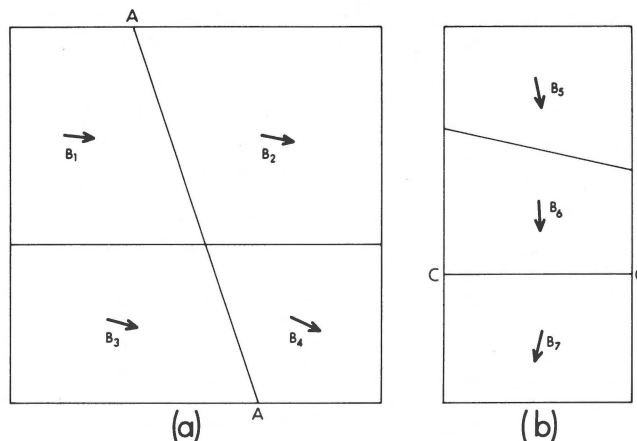


Fig. 4(a) Map of an area consisting of four domains with fold-axes $B_1 \ B_2 \ B_3 \ B_4$. A composite vertical section of variable obliquity may be constructed along the line AA using four computer plots, one for each domain. (b) Map of an area consisting of three domains with fold-axes $B_5 \ B_6 \ B_7$. A composite vertical section cannot be constructed along the line CC using three plots, one for each domain, because in the case of domain 5 the outcrops would have to be projected parallel to B_5 across domain 6 where the fold-axis is B_6 .

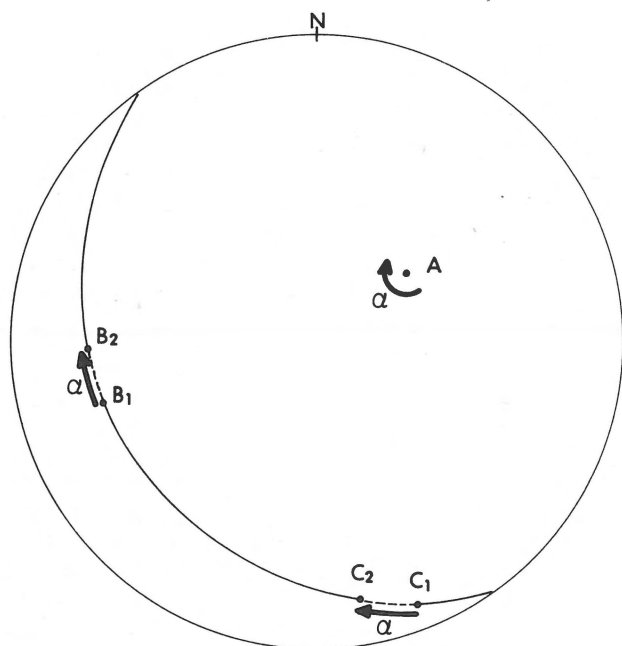


Fig. 5
Stereographic projection illustrating the principles of rotation of domain 1 so that its fold-axis B_1 coincides with B_2 , the fold-axis in domain 2. This rotation should take place about an axis A that is normal to the plane containing B_1 and B_2 . The coordinates of outcrops in domain 1 are first referred to the mutually perpendicular axes AB_1C_1 . These coordinates are the same as those referred to the mutually perpendicular axes AB_2C_2 after domain 1 has been rotated so that B_1 coincides with B_2 . The AB_2C_2 coordinates are then referred back to conventional north, east and vertical axes.

cosines of A and B_1 and A and B_2 , respectively. Let M be a $3 \times p$ matrix whose columns are the coordinates of the outcrops in domain 1 referred to conventional axes, let M_1 be the equivalent matrix where the reference axes are AB_1C_1 and let D_1 be a 3×3 matrix whose rows are the direction cosines of AB_1C_1 . Now M_1 obtained through premultiplying M by D_1 , also gives the coordinates of the outcrops in domain 1, referred to axes AB_2C_2 , after this domain has been rotated so that B_1 coincides with B_2 . All that then remains to be done to complete the rotation is to refer these coordinates back to the conventional axes. This can be accomplished by premultiplying M_1 by the 3×3 matrix D_2 whose columns are the direction cosines of AB_2C_2 . Thus the complete rotation can be carried out using the matrix multiplication

$$[M_2] = [D_2] [D_1] [M] \quad (10)$$

where M_2 is a $3 \times p$ matrix whose columns are the coordinates of the outcrops in domain 1, after this domain has been rotated so that B_1 coincides with B_2 . Before rotation the coordinates of domain 1 should be referred to an origin half-way along the boundary between the two domains. Only in this way will a large discontinuity not come to exist between the rotated outcrops of domain 1 and the unrotated outcrops of domain 2 (fig. 6). A slight

overlap and gap will always occur, but as long as the rotations are small, say less than 20° , these will not be significant. If the coordinates of the new origin are $[a \ b \ c]$, the new coordinates of the outcrop $[x \ y \ z]$ are $[x-a \ y-b \ z-c]$.

Bearing in mind that the direction cosines of a line are also the coordinates of a point on a line unit distance from the origin, the direction cosines of the s -poles in domain 1 can be rotated in the same way as the coordinates. Once the coordinates and direction cosines of s -poles in domain 1 have been transformed, i.e., the domain has been rotated, the whole area may be considered as a single domain with B_2 as its fold-axis, and computer plots for construction sections obtained by the usual procedure.

STRUCTURE OF THE REMOUCHAMPS AREA

In this study of the structure of the Remouchamps area we used orientation data from 215 outcrops, one reading per outcrop, that had been collected by students attending University of Amsterdam field schools. The coordinates of each outcrop were measured to the nearest 10 m; the first two coordinates refer to the distances east and north of the base-station shown on figure 7 and the third coordinate to the elevation above sea-level. Bedding planes are commonly difficult to recognize and measure in the shales of unit C so orientation data from this unit were not used to estimate fold-axes and to test for cylindricity.

The area was divided into five subareas whose boundaries were approximately those between the domains shown in figure 7. At each of 41 limestone and sandstone outcrops, 10 measurements of bedding were recorded. The concentration parameter calculated from these readings does not vary significantly from one lithology to the other; the mean value was found to be 192. The matrix T (eq. 2) was then compiled for each subarea and its smallest eigenvalue λ_3 calculated. These

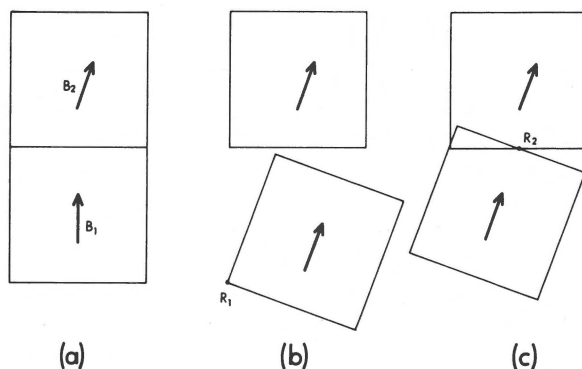


Fig. 6(a)
Map of an area with domains 1 and 2 where fold-axes are B_1 and B_2 , respectively. (b) Map showing the large discontinuity (gap) that develops after domain 1 has been rotated about an axis passing through R_1 , a point not on the boundary between the two domains. (c) Map showing the small discontinuity (gap and overlap) that develops when the axis of rotation passes through R_2 , a point on the boundary between the two domains.

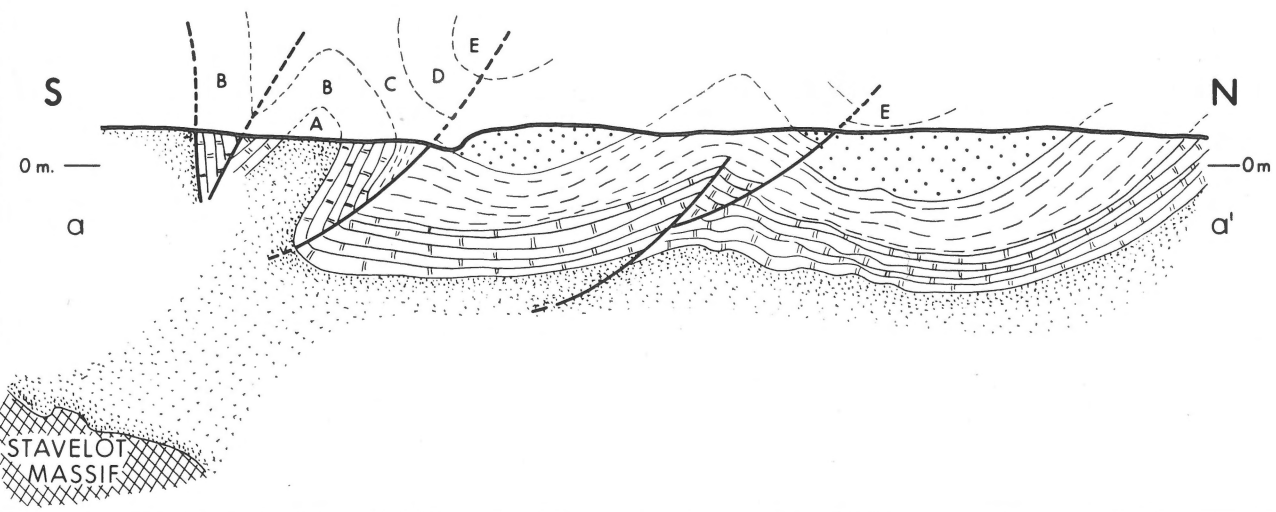
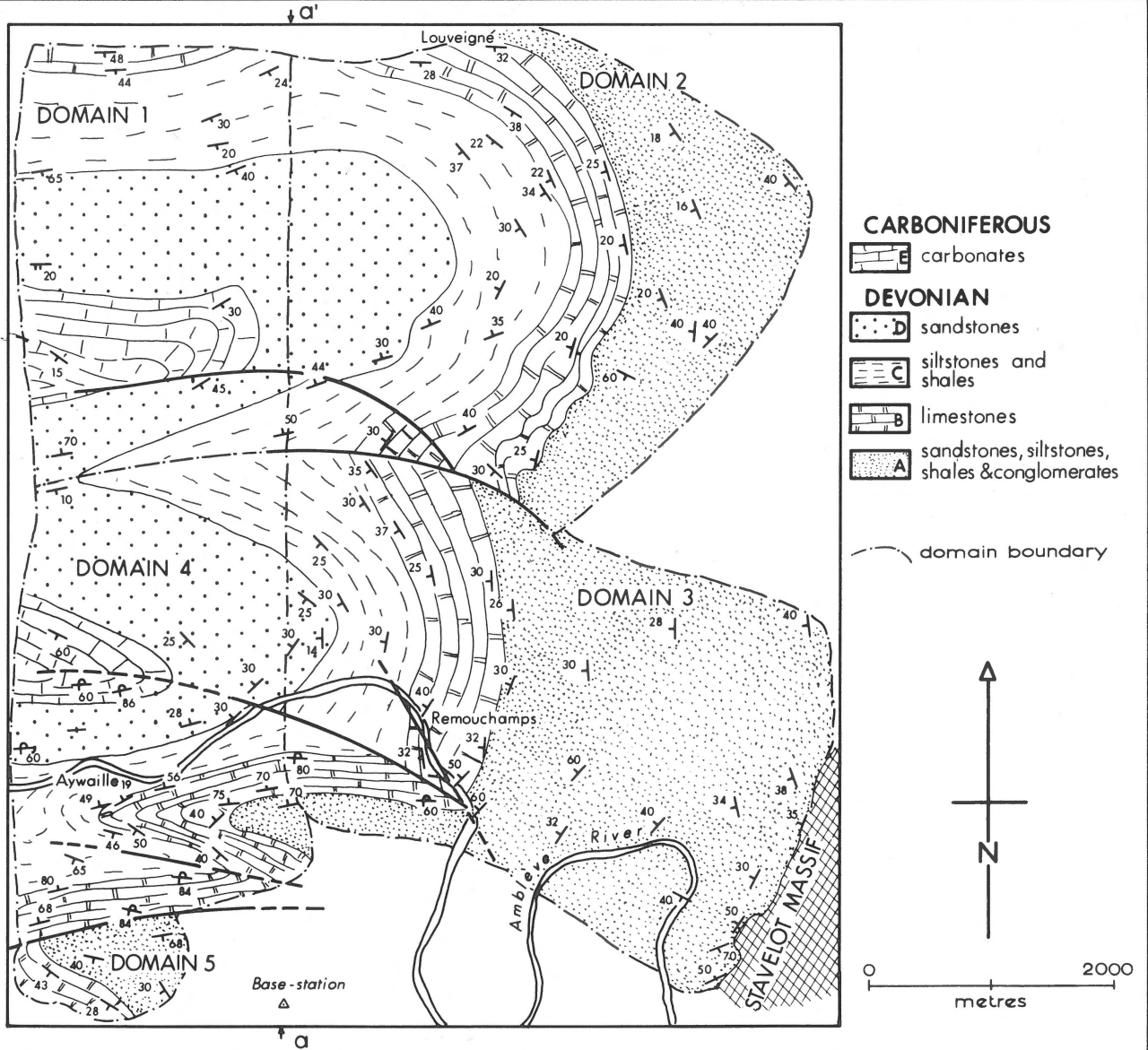


Fig. 7
 Reinterpreted geological map and vertical cross-section of the Remouchamps area. The map shows the relative positions of the five domains into which the area has been divided. The cross-section was constructed from four computer-plots that show the projections of each outcrop in domains 1-4 parallel to the appropriate fold-axis onto a vertical plane along the line aa'.

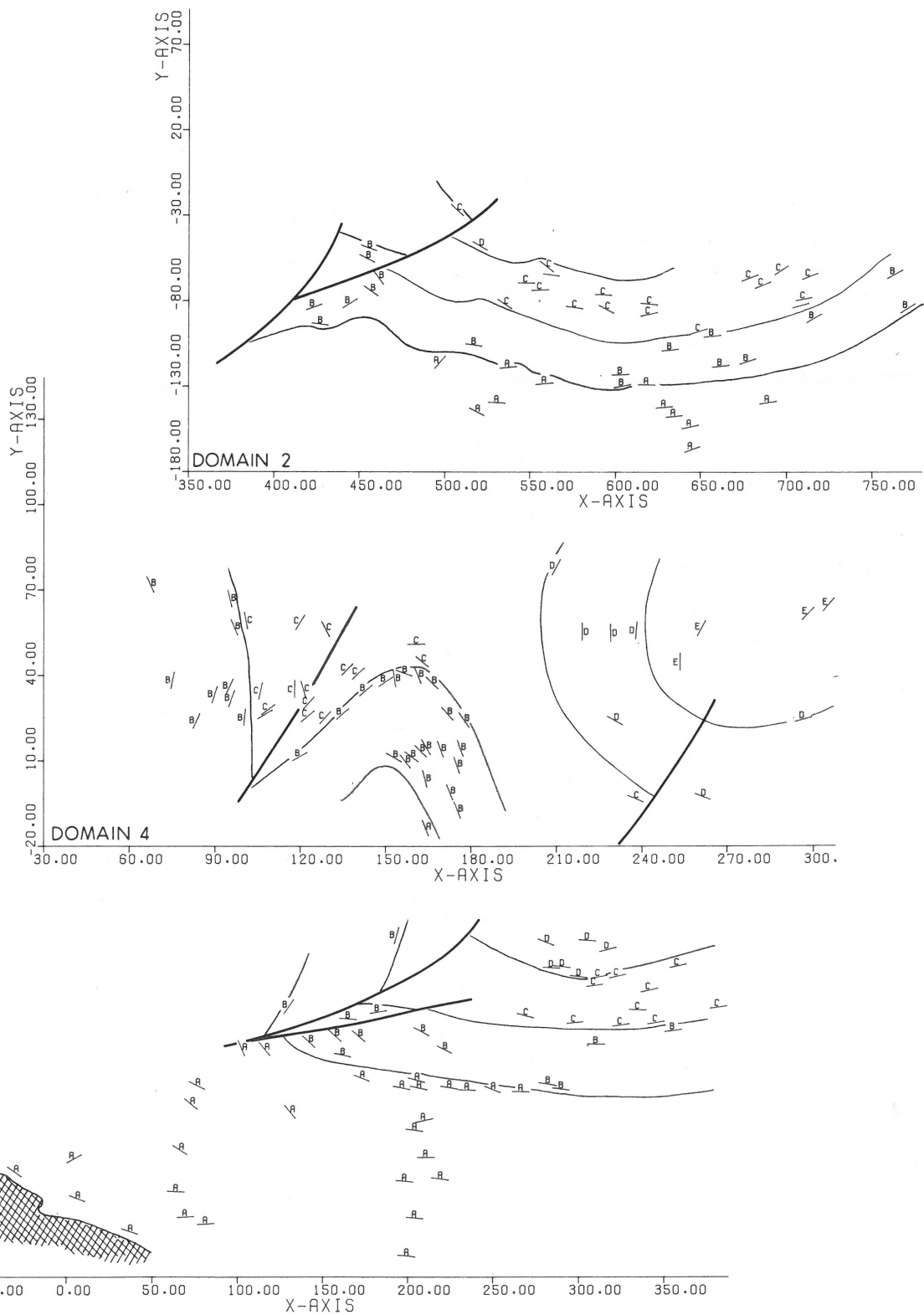


Fig. 8

Profiles through domains 2 (top), 4 (centre) and 3 (bottom) of the Remouchamps area. For descriptions of units A-E see fig. 2. The short lines are computer-plotted traces of bedding. The contacts between units have been drawn by hand as have the traces of faults. The steep transverse fault near Remouchamps is the lower of the two faults shown in the profile for domain 3. The origin of each profile is the projection of the basestation shown in fig. 7. The x- and y-values are in tens of metres.

values of λ_3 and the above value of K were then substituted in equation 3 and in each case the value of $K \lambda_3$ was greater than the appropriate value of χ^2 . Thus the null hypothesis of coplanarity was rejected for each of the five subareas, thereby indicating that the scatter of bedding poles about the best-fit plane cannot be accounted for by measurement and small-scale roughness errors alone. Each of the subareas was then divided into two segments, λ_3 of the matrix T determined for each segment and the value of the statistic for use in the coaxiality test (eq. 4) calculated. In each case this statistic was less than the appropriate value of F. We therefore conclude that the scatter of bedding-poles in each subarea can be accounted for by errors associated with measurement and with small- and large-scale roughness features, so that each subarea may be regarded as a domain within which folding is statistically cylindrical. The large-scale roughness features may be related to faults or to phases of deformation younger than the one during which the macroscopic folding occurred. After using the methods described above to eliminate spurious data and refine the boundaries between domains, the fold-axes (λ_3 eigenvectors) for each domain were recalculated and found to be (1) 255 3, (2) 266 21, (3) 256 28, (4) 269 25, and (5) 253 28. The average value of λ_3 divided by the number of readings was found to be 0.0151 which indicates that the standard deviation of the angles between the bedding-poles and the appropriate best-fit plane is about 7° .

From an input of [x y z] coordinates, bedding-plane orientations and stratigraphic unit identifications, a computer plot was obtained for each domain that shows the projection of each outcrop as well as the trace of bedding on a plane normal to the fold-axis. Lines representing the traces of the contacts between the stratigraphic units as well as faults were drawn by hand on these plots three of which are shown in figure 8.

A composite vertical cross-section along the line aa' of figure 7 was prepared using four computer plots not reproduced here which had to be fitted together manually. This section is not completely accurate since each of the plots is on a plane oblique to the fold-axis, the degree of obliquity varying from one plot to the other. Furthermore domain 5 could not be projected because it is not on the line of section.

Due to the above disadvantages a composite section was constructed by rotating domains as follows. First, representative outcrops were selected from each domain: the use of all the outcrops would have resulted in too high a density of points on the computer plot. These outcrops are shown in figure 7. Domains 1, 2, 3 and 5 were then rotated so that their fold-axes B_1 B_2 B_3 and B_5 became parallel to B_4 , the fold-axis in domain 4.

Domain 3 was rotated such that B_3 coincided with B_4 . For the purposes of this rotation, the outcrop coordinates in domain 3 were transformed to an origin half-way along the boundary between it and domain 4. The rotational matrices D_1 and D_2 and the matrix M of direction cosines of bedding-

poles and transformed outcrop coordinates in domain 3 were then constructed as described above and the matrix multiplications specified in equation 10 carried out. The direction cosines and coordinates specified by product M_2 of these multiplications were added to the direction cosines of bedding-poles and outcrop coordinates in domain 4.

Because the prominent syncline in domain 2 is apparently continuous with that in domain 1, we decided to adopt a rotational procedure that minimizes the rotational discontinuity between these domains. Thus, although domains 2 and 5 were treated in a manner similar to domain 3, domain 1 was first rotated about an origin half-way along the boundary between it and domain 2, such that B_1 came to coincide with B_2 . The rotated domain 1 was then rotated along with domain 2 such that B_2 came to coincide with B_4 . The discontinuity between domains 1 and 2 created by following this procedure is smaller than that produced by rotating domains 1 and 2 independently.

Once the direction cosines of bedding-poles and the coordinates of outcrops in domains 1, 2, 3 and 5 had been transformed as described above, the whole area could be considered as a single domain with B_4 as its fold-axis. A computer plot for a plane normal to B_4 was then obtained in the usual manner (fig. 9).

The composite sections of figures 7 and 9, as well as having greater vertical range, differ from those of Fourmarier (fig. 1) in two ways. First, the folds in units D and E are more rounded in our sections, thereby implying that the disharmony between these units and the underlying levels is not as important as previously thought: only south of the Amblève River does the incompetent unit C begin to act as a decoupling level between the overlying and underlying competent units. Secondly, the thrust-faults in our sections make smaller angles with the bedding and appear to flatten with depth; of the three faults shown in the southern part of domain 4, the presence of the most northerly is based solely on the cross-sections. The steep transverse fault near Remouchamps shown on the maps of figures 1 and 7 projects as a low-angle fault in section (fig. 8, domain 3; fig. 9); it is not shown in the section of figure 7 because it does not intersect the line of section.

The thickness of unit B-D as revealed by the profiles of individual domains varies considerably from one part of the area to another: units C and D in the northern limbs of synclines are considerably thicker than elsewhere. Such thickening could well be tectonic in origin, caused for example by low-angle thrust faulting, but variations in the original stratigraphic thickness are common throughout the eastern end of the Dinant synclinorium.

The cross-sections of figures 7 and 9 provide evidence of the northward movement of units B-E, affected by folding and thrusting, with respect to the Stavelot massif. Unit A, which has not been affected by folding to the same extent as the overlying units, may be considered as a thick basal zone of disharmony between the Stavelot massif and the overlying sedimentary cover (see e.g. B r e d d i n, 1973).

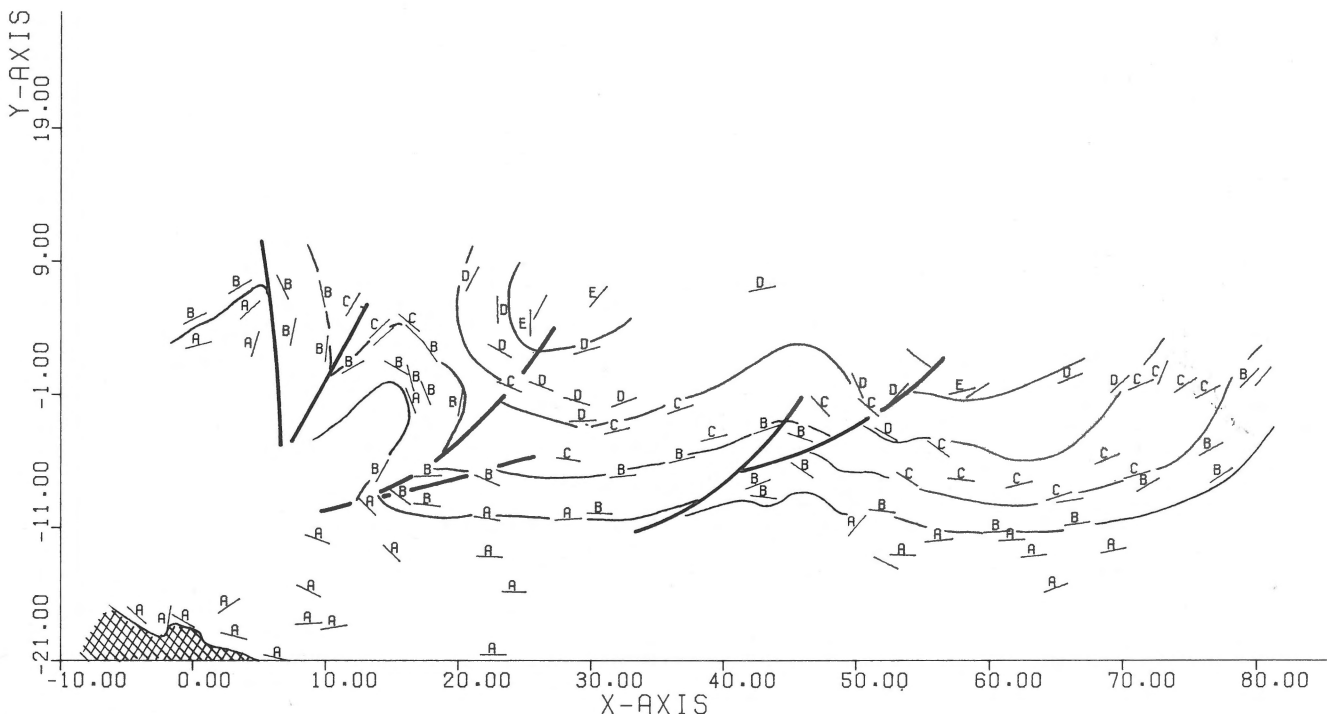


Fig. 9

Composite profile of the Remouchamps area looking down the fold-axis (269 25) in domain 4. Domains 1, 2, 3 and 5 have been rotated so that their fold-axes coincide with the fold-axes in domain 4. The short lines are computer-plotted traces of bedding. The contacts of units have been drawn by hand as have the traces of faults. The origin of the profile is the projection of the base-station shown in fig. 7. The x- and y-values are in hundreds of metres.

ACKNOWLEDGEMENTS

One of us (H.A.K. Charlesworth) gratefully acknowledges the award of research grants from the National Research Council of Canada and the Geological Survey of Canada which were used to defray computing costs. Mr. S. Verburgh acted as field assistant. Dr. J. Ramsden helped with the computing and Messrs. G.R. Dales and T. Bojczyszyn with some of the data gathering.

REFERENCES

- Asselberghs, E. (1946) – L'Eodévonien de l'Ardenne et des régions voisines. *Mém. Inst. Géol. Univ. Louvain*, 14.
- Bouckaert, J., M. Strel & J. Thorez (1970) – Zur biostratigraphischen Gliederung und zu den Referenz-Schichten des Famenniums in Belgien. *Zeitschr. deutsch. Geol. Gesellschaft*, 120, p. 238-291.
- Breidin, H. (1973) – Tiefentektonik und Deckenbau im Massiv von Stavelot-Venn (Ardennen und Rheinisches Schiefergebirge). *Geol. Mitt.*, 12, p. 81-130.
- Charlesworth, H.A.K., C.W. Langenberg & J. Ramsden (1976) – Determining axes, axial planes, and sections of macroscopic folds using computerbased methods. *Can. J. Earth Sci.*, 13, p. 54-65.
- Coen, M. (1974) – Le Frasnien de la bordure orientale du bassin de Dinant. *Ann. Soc. Géol. Belg.*, 97, p. 67-103.
- Fourmarier, P. (1952) – Trois coupes méridiennes dans la terminaison nord-orientale du synclinorium de Dinant. *Ann. Soc. Géol. Belg.*, 75, p. B167-174.
- , (1954) – Prodomme d'une description géologique de la Belgique. *Mém. Soc. Géol. Belg.*, Brussels, 826 pp.
- , (1958) – Carte géologique de la Belgique, 1 : 25,000, Feuille Louveigné-Spa 148 (with explicative text).
- Kelker, D. & C.W. Langenberg, (1976) – A mathematical model for orientation data from macroscopic cylindrical folds. *J. Math. Geol.*, 8, p. 549-561.
- Mardia, K.V. (1972) – *Statistics of Directional Data*. Academic Press, London, 357 pp.